JOURNAL OF VIROLOGY, Oct. 2007, p. 11520–11525 Vol. 81, No. 20
0022-538X/07/$08.00+0 doi:10.1128/JVI.01308-07

NOTES

Enhancement of Murine Coronavirus Replication by Severe Acute Respiratory Syndrome Coronavirus Protein 6 Requires the N-Terminal Hydrophobic Region but Not C-Terminal Sorting Motifs▽

Jason Netland,[1] Debra Ferraro,[2] Lecia Pewe,[2] Heidi Olivares,[3] Thomas Gallagher,[3] and Stanley Perlman[1,2]*

Interdisciplinary Program in Immunology[1] and Department of Microbiology,[2] University of Iowa, Iowa City, Iowa, and Department of Microbiology and Immunology, Loyola University Medical Center, Maywood, Illinois[3]

Received 14 June 2007/Accepted 23 July 2007

Severe acute respiratory syndrome coronavirus encodes several accessory proteins of unknown function. We previously showed that one such protein, encoded by ORF6, enhanced the growth of mouse hepatitis virus in tissue culture cells and in mice. Protein 6 consists of an N-terminal hydrophobic peptide and a C-terminal region containing intracellular protein sorting motifs. Herein, we show that mutation of the hydrophobic region but not the sorting motifs affected the ability of protein 6 to enhance virus growth. Collectively, these results support the notion that the 6 protein interacts with membrane-bound viral replication or assembly machinery to directly enhance virus replication and virulence in animals.

The etiological agent of the severe acute respiratory syndrome (SARS) was identified as a coronavirus (SARS-CoV). In additional to structural proteins, SARS-CoV encodes eight accessory proteins, whose functions are not well defined (15). Previously, we introduced each of the SARS-CoV accessory genes into an attenuated strain of mouse hepatitis virus (MHV), strain JHM J2.2-v-1, (J2.2-v-1), by using reverse genetics (14). J2.2-v-1 causes a mild encephalitis followed by a chronic demyelinating encephalomyelitis (4). The expression of only the SARS-CoV ORF6 gene, of all the genes evaluated, resulted in a gain of function. Mice infected with MHV expressing ORF6 (strain rJ2.2.6) exhibited greater mortality and morbidity and higher virus titers than mice infected with control viruses harboring a nonfunctional ORF6 gene (designated rJ.2.2.6^{KO}) (14).

The sequence of protein 6 suggests that it is composed of two distinct regions (Fig. 1A). The N-terminal portion extends through residue 38 and is composed primarily of hydrophobic residues, with six interspersed charged residues spaced roughly seven residues apart, suggesting an amphipathic alpha-helical structure Fig. 1B. The C-terminal region is hydrophilic and contains the sequence YSEL, which can target a protein for internalization from the cell membrane to the endosomal/lysosomal compartments (1, 6, 8, 19), and four diacidic sequences (DxE), which can mediate exit from the endoplasmic reticulum (12). Herein, we examine whether the N-terminal amphipathic portion or the putative protein sorting motifs in the C terminus are essential for protein 6 to influence CoV infections.

As in our previous studies, we used J2.2-v-1 as the parental virus (13). Variants were generated by PCR using primers encoding the desired ORF6 mutations (primer sequences available upon request). In the first set of mutants, YSEL and diacidic sorting motifs located near the C terminus were changed to alanines (Fig. 1). In one virus [rJ2.2.6$^{0(DxE)}$], all of the sorting motifs were mutated, whereas in a second one [rJ2.2.6$^{1(DxE)}$], the most distal diacidic motif was retained. In the second set, portions of the N-terminal hydrophobic region, encompassing residues 3 to 10 (rJ2.2.6$^{\Delta 3\text{-}10}$), 11 to 18 (rJ2.2.6$^{\Delta 11\text{-}18}$), or 3 to 18 (rJ2.2.6$^{\Delta 3\text{-}18}$), were deleted (Fig. 1C). Each mutant protein also contained a C-terminal hemagglutinin (HA) tag to facilitate detection. Recombinant MHV containing ORF6 variants were generated by targeted recombination as previously described (11, 14). Two independent isolates were generated by two rounds of plaque purification from two independent rescue experiments for each ORF6 variant virus. The two isolates behaved indistinguishably, so results from both were combined in all experiments. As controls, we used virus expressing wild-type protein 6 (rJ2.2.6) and rJ.2.2.6^{KO}, which included ORF6 but lacked expression due to mutation of the initiator methionine and insertion of a termination codon at position 27 (14). Expression of the various forms of protein 6 was confirmed by Western blot assay as previously described (Fig. 1D) (14). Of note, the mobilities of the N-terminal-deleted proteins were identical to that of the intact protein. These unusual electrophoretic mobilities were also observed for wild-type and variant proteins expressed from plasmid DNAs (data not shown).

* Corresponding author. Mailing address: Department of Microbiology, University of Iowa, BSB 3-712, Iowa City, IA 52242. Phone: (319) 335-8549. Fax: (319) 335-9999. E-mail: stanley-perlman@uiowa.edu.

▽ Published ahead of print on 1 August 2007.

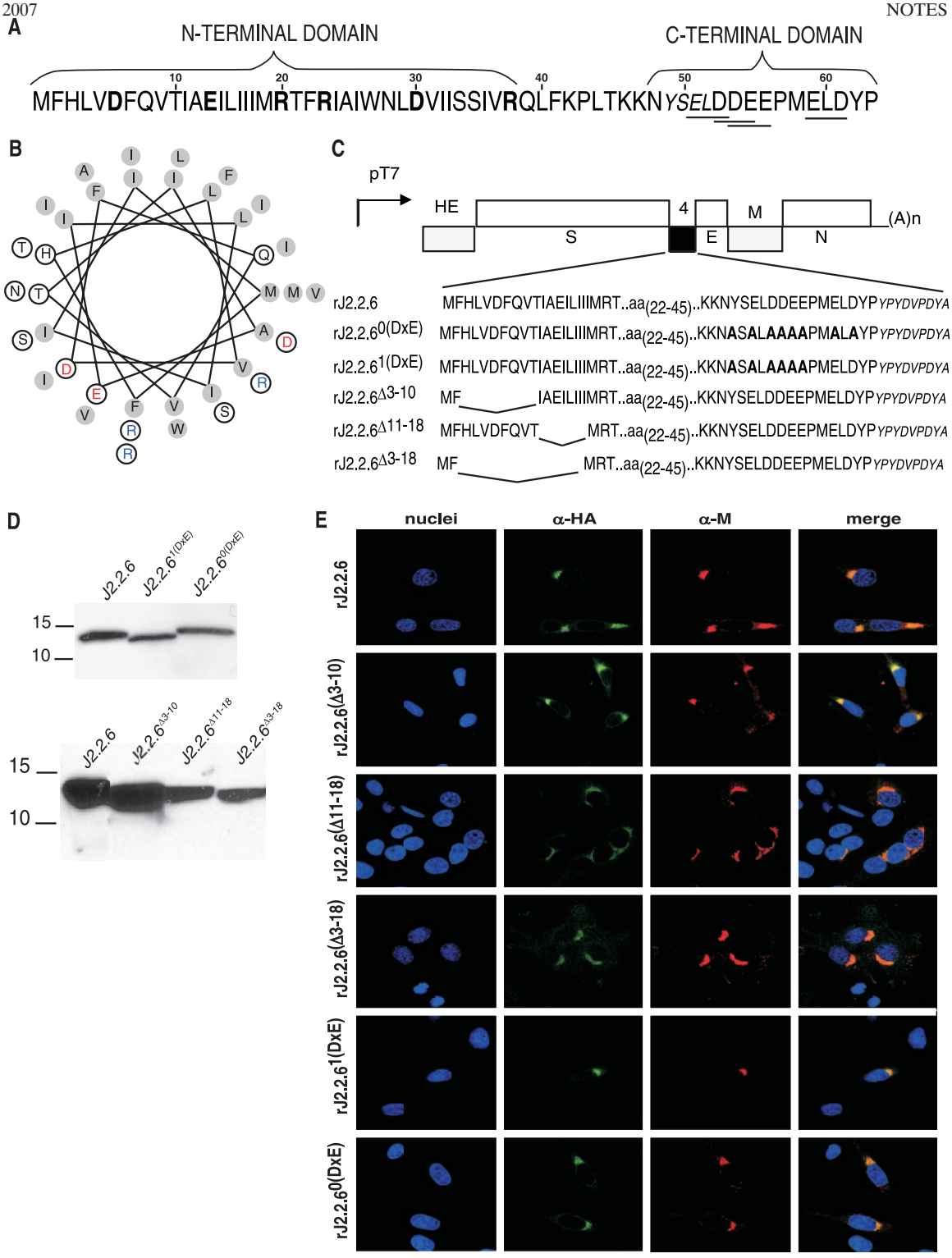

FIG. 1. Generation of rJ2.2 expressing SARS-CoV ORF6 variants. (A) Amino acid sequence of protein 6 showing the N-terminal amphipathic portion with interspersed charged residues (boldface) and the C terminus containing a tyrosine sorting motif (italics) and four diacidic motifs (underlining). (B) Helical wheel projection of the predicted N-terminal amphipathic helix (residues 1 to 38). Shaded and open circles indicate hydrophobic and hydrophilic residues, respectively. Red and blue letters indicates acidic and basic residues, respectively. (C) Protein 6 variants containing alanine substitutions to abrogate the function of the sorting motifs or deletions within the hydrophobic portion were generated and introduced into ORF4 of rJ2.2 by targeted recombination as previously described (14). HE, hemagglutinin-esterase; S, spike; E, envelope; M, transmembrane; N, nucleocapsid. (D) Virally encoded protein 6 variants were detected by Western blot assay using anti-HA MAb HA.11 (Covance, Berkeley, CA). (E) Confocal microscopy of 17Cl-1 cells infected with J2.2.6 and all variant viruses. Cells were infected at a multiplicity of infection of 0.1, fixed at 10 to 11 h postinfection, and stained with mouse anti-MHV M MAb (MAb 5B11.5; provided by M. Buchmeier, The Scripps Research Institute, La Jolla, CA) and fluorescein isothiocyanate-conjugated rat anti-HA (MAb 3F10; Roche Molecular Biochemicals, Mannheim, Germany) to detect protein 6. Nuclei were labeled with TO-PRO3 (Invitrogen, Carlsbad, CA).

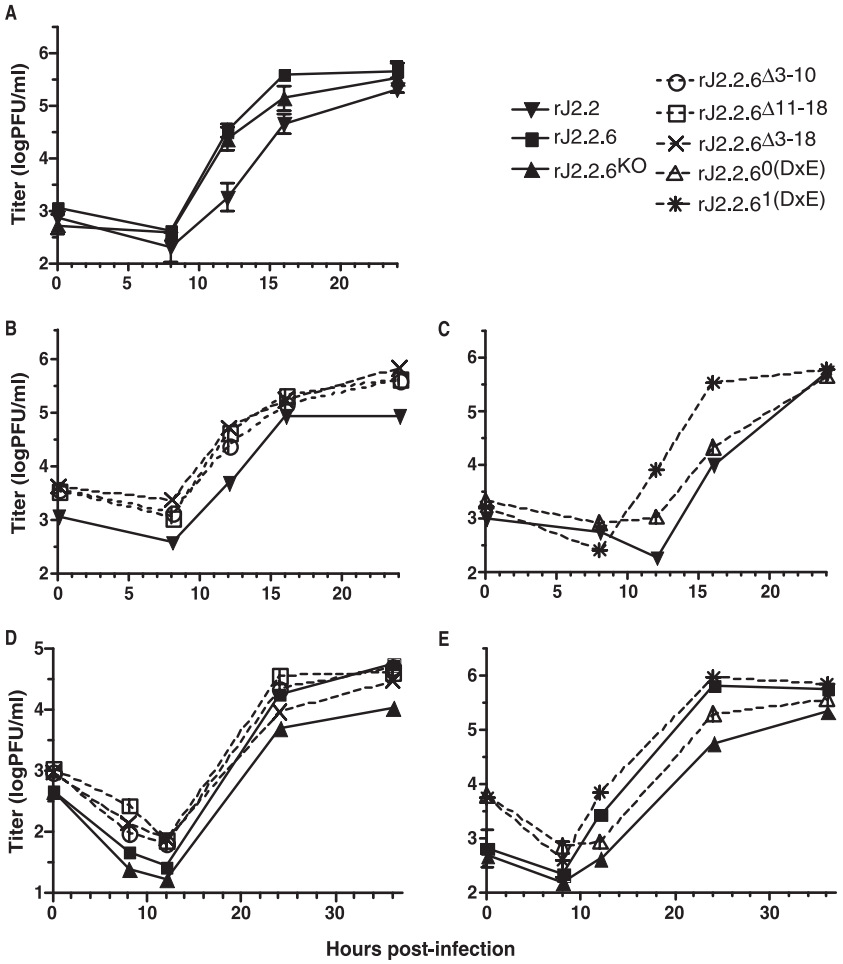

FIG. 2. Virus titers in cells infected with rJ2.2 expressing mutated SARS-CoV protein 6. (A to C) 17Cl-1 cells were infected (multiplicity of infection, 1.0) in triplicate with (A) rJ2.2, J2.2.6 or J2.2.6^{KO}, or (B) J2.2, rJ2.2.6$^{\Delta 3\text{-}10}$, rJ2.2.6$^{\Delta 11\text{-}18}$, or rJ2.2.6$^{\Delta 3\text{-}18}$ or (C) J2.2, rJ2.2.6$^{0(DxE)}$, or rJ2.2.6$^{1(DxE)}$. (D and E) L929 cells were infected with (D) rJ2.2.6, rJ2.2.6^{KO}, rJ2.2.6$^{\Delta 3\text{-}10}$, rJ2.2.6$^{\Delta 11\text{-}18}$ or rJ2.2.6$^{\Delta 3\text{-}18}$ or (E) rJ2.2.6, rJ2.2.6^{KO}, rJ2.2.6$^{0(DxE)}$, and rJ2.2.6$^{1(DxE)}$. Cells were harvested at the indicated times, and viral titers were determined by plaque assay on HeLa-MHVR cells. Error bars are included but are too small to be visible.

To determine whether the various protein 6 variants influenced virus growth in tissue culture cells, we assayed the kinetics of viral replication in 17Cl-1 cells, a cell line that is highly susceptible to MHV infection. 17Cl-1 cells were infected in triplicate with rJ2.2, rJ2.2.6, rJ2.2.6^{KO} and the 6 protein variant viruses, harvested at various times postinfection (p.i.), and titered on HeLa cells expressing the cellular receptor for MHV (HeLa-MHVR cells). rJ2.2 (wild-type recombinant virus), rJ2.2.6, and rJ2.2.6^{KO} exhibited similar growth kinetics in these cells (Fig. 2A). All viruses expressing mutant ORF6 genes grew at least as well as rJ2.2 in 17Cl-1 cells (Fig. 2B and C) but, remarkably, rJ2.2.6$^{1(DxE)}$, containing only a single residual diacidic sorting motif, exhibited more rapid growth kinetics (Fig. 2C).

We also assayed the kinetics of virus replication in L929 cells, because protein 6 enhances the kinetics of rJ2.2.6 growth in these cells (14, 16). We infected L929 cells in triplicate with rJ2.2.6, rJ2.2.6^{KO}, or rJ2.2 encoding mutated protein 6 (Fig. 2D and E). In agreement with our previous results, rJ2.2.6 grew to higher titers than rJ2.2.6^{KO} (14). All five mutant viruses, like J2.2.6, grew more efficiently in L929 cells than did rJ2.2.6^{KO} (Fig. 2). Of note, rJ2.2.6$^{1(DxE)}$, which grew more rapidly in 17Cl-1 cells than any of the other viruses, replicated to only marginally higher titers in L929 cells (Fig. 2E).

Since the YSEL and DxE motifs are important in protein subcellular localization, we next examined whether mutation of these motifs, or of the N-terminal hydrophobic domain, alters 6 protein localization. To achieve this, we used confocal microscopy to simultaneously examine the localization of protein 6 and J2.2-v-1 M protein, which localizes to the Golgi membranes at sites of virus assembly and exhibits extensive overlap with wild-type protein 6 (14). 17Cl-1 cells were infected with recombinant viruses and processed as described previously (14). As demonstrated in Fig. 1E, native protein 6, 6$^{1(DxE)}$-HA, and 6$^{0(DxE)}$-HA all displayed similar overlap with M proteins. Furthermore, deletion of portions of the N terminus did not alter protein 6 localization, as 6$^{\Delta 3\text{-}10}$-HA, 6$^{\Delta 11\text{-}18}$-HA, and 6$^{\Delta 3\text{-}18}$-HA all exhibited near-complete colocalization with M protein. These results indicate that residues other than 3 to 18

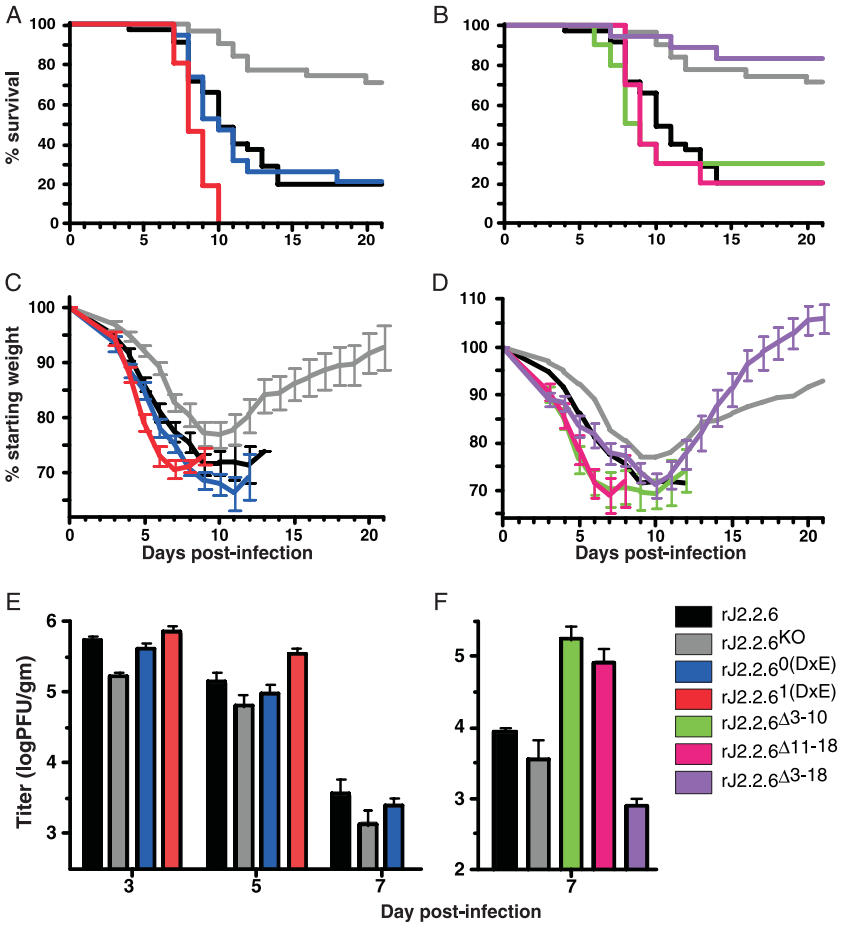

FIG. 3. Morbidity, mortality, and viral titers in infected mice. B6 mice were infected intranasally with 1,000 PFU of protein 6 variant viruses or controls and monitored daily for mortality (A and B) and weight loss (C and D). (A and C) Mortality (A) and weight loss (C) after infection with rJ2.2.6 ($n = 35$), rJ2.2.6^{KO} ($n = 31$), or viruses expressing protein 6 with mutated sorting motifs [rJ2.2.6$^{0(DxE)}$ ($n = 19$) or rJ2.2.6$^{1(DxE)}$] ($n = 26$). (B and D) Mortality (B) and weight loss (D) after infection with rJ2.2.6, rJ2.2.6^{KO}, or viruses expressing 6 protein with hydrophobic domain deletions (rJ2.2.6$^{\Delta 3\text{-}10}$ [$n = 10$], rJ2.2.6$^{\Delta 11\text{-}18}$ [$n = 10$], or rJ2.2.6$^{\Delta 3\text{-}18}$ [$n = 18$]). (E and F) Viral titers in brain homogenates from infected mice were determined by plaque assay on HeLa-MHVR cells. (E) Virus titers in mice infected with rJ2.2.6 ($n = 5$), rJ2.2.6$^{1(DxE)}$ ($n = 5$), or rJ2.2.6$^{0(DxE)}$ ($n = 5$) were greater than those infected with rJ2.2.6^{KO} ($n = 5$) ($P < 0.01$) at day 3 p.i. Titers for rJ2.2.6$^{1(DxE)}$-infected mice ($n = 7$) were greater than those infected with rJ2.2.6 ($n = 5$), rJ2.2.6^{KO} ($n = 5$), or rJ2.2.6$^{0(DxE)}$ ($n = 10$) at day 5 p.i. ($P < 0.05$). (F) Titers in the brains of mice infected with rJ2.2.6$^{\Delta 3\text{-}18}$ ($n = 4$) were significantly lower than those found for mice infected with rJ2.2.6 ($n = 5$), rJ2.2.6$^{\Delta 3\text{-}10}$ ($n = 6$), or rJ2.2.6$^{\Delta 11\text{-}18}$ ($n = 4$) at day 7 p.i. ($P < 0.01$).

and the putative protein sorting motifs are responsible for directing the subcellular localization of protein 6.

Our previous studies demonstrated that rJ2.2.6 was highly lethal in mice compared to infection with rJ2.2 or rJ2.2.6^{KO}. The increased lethality was accompanied by increased viral titers in the brains (14). To determine the importance of the sorting motifs and hydrophobic domain in protein 6-mediated disease enhancement, we infected mice intracranially with 1,000 PFU of rJ2.2.6, the protein 6 variant viruses, or the control virus rJ2.2.6^{KO} and monitored them for weight loss and mortality. Mice infected with rJ2.2.6$^{0(DxE)}$, encoding a protein 6 lacking all sorting motifs, with rJ2.2.6$^{\Delta 3\text{-}10}$ and rJ2.2.6$^{\Delta 11\text{-}18}$, each lacking eight amino acids of the hydrophobic domain, and with rJ2.2.6 displayed nearly identical weight loss kinetics and mortality (Fig. 3). Consistent with the enhanced kinetics of virus growth in 17Cl-1 cells (Fig. 2A), mice infected with rJ2.2.6$^{1(DxE)}$, which retains only a single diacidic motif, displayed more rapid lethality than those infected with rJ2.2.6 (Fig. 3A and C). Notably, 6$^{\Delta 3\text{-}18}$ protein did not enhance mortality, as infection with rJ2.2.6$^{\Delta 3\text{-}18}$ resulted in disease similar to that observed for rJ2.2.6^{KO}-infected mice (Fig. 3B and D).

To further investigate the basis of these differences in virulence, we measured titers in the brains of mice infected with the various recombinant viruses by plaque assay using HeLa-MHVR cells (Fig. 3E). At day 3 p.i., virus titers in mice infected with rJ2.2.6, rJ2.2.6$^{0(DxE)}$, and rJ2.2.6$^{1(DxE)}$ were similar to one another and were significantly higher than those found in rJ2.2.6^{KO}-infected mice ($P < 0.01$). Virus titers were higher in rJ2.2.6$^{1(DxE)}$-infected mice than in mice infected with rJ2.2.6 at day 5 p.i. ($P < 0.05$), consistent with the enhanced clinical disease. Titers could not be evaluated at day 7 p.i. in rJ2.2.6$^{1(DxE)}$-infected mice, as most had succumbed to infection by this time. The basis for this increase in virus titers and mortality is not known, since rJ2.2.6$^{1(DxE)}$ showed no differences in localization (Fig. 1E) or levels of expression (Fig. 1D). Titers in the brains of mice infected with rJ2.2.6, rJ2.2.6$^{0(DxE)}$,

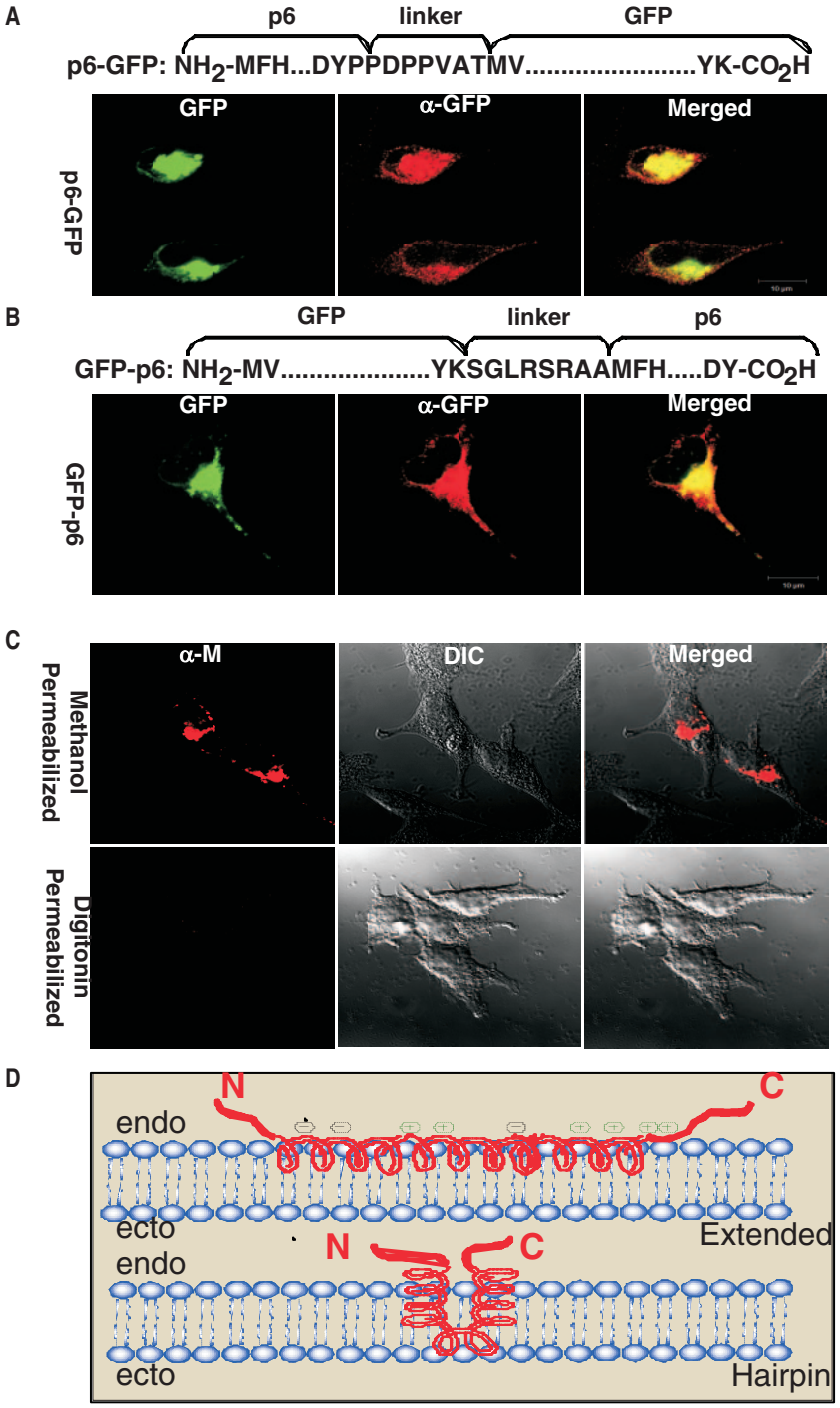

FIG. 4. Subcellular positions of GFP appends on protein 6-GFP and GFP-protein 6 chimeras. HeLa cells were transfected with plasmids encoding p6-GFP (A) or GFP-p6 (B) and photographed 24 h later by confocal microscopy. Panels depict GFP fluorescence (left), positions of anti-GFP (α-GFP) antibodies after digitonin permeabilizations (middle), and a merging of the two images (right). Images in part C depict 293 cells transfected 24 h earlier with plasmids encoding MHV strain A59 M proteins. Cells were permeabilized with methanol (top panels) or digitonin (bottom panels) and incubated with anti-M (α-M) antibody J.1.3 (provided by J. Fleming, University of Wisconsin, Madison, WI), which binds an epitope in Golgi lumen (2, 3). Photographs reveal immunofluorescent (left), differential interference contrast (DIC; middle), and merged images (right). These experiments were conducted three times with identical results. Part D schematizes two putative configurations of protein 6 relative to intracellular membranes. endo, cytoplasmic; ecto, luminal.

rJ2.2.6$^{\Delta 3\text{-}10}$, or rJ2.2.6$^{\Delta 11\text{-}18}$ were significantly higher ($P < 0.01$) than those detected for mice infected with rJ2.2.6$^{\Delta 3\text{-}18}$ or rJ2.2.6^{KO} at 7 days p.i. (Fig. 3E).

Given that sequences near protein 6 termini were evaluated for their effects on virus growth and virulence, we addressed whether their termini might project into the cytosol. ORF6 appended with green fluorescent protein (GFP)-encoding sequences at either terminus were synthesized in HeLa cells from

plasmid DNAs and evaluated by immunofluorescence microscopy. Intracellular localizations for the GFP tags (Fig. 4A and B) were similar to those observed for HA-tagged protein 6 (Fig. 1E). Digitonin permeabilizations permitted access of anti-GFP antibodies, which bound to both GFP-p6 and p6-GFP, arguing for cytosolic positions of both the N- and C-terminal appends. The same digitonin permeabilizations did not allow MHV M protein antibodies (monoclonal antibody [MAb] J.1.3, recognizing luminal epitope) to transfer into the organelle lumen of intracellular membranous organelles (Fig. 4C).

These findings indicate that protein 6 can adopt an unusual N-cytoplasmic:C-cytoplasmic configuration, but they do not rule out an N-luminal:C-cytoplasmic form for a native protein lacking N-terminal GFP. The N-terminal portion is both amphipathic (Fig. 1B) and membrane associated. If the N-terminal portion is alpha-helical, then protein 6 may adopt a hairpin or extended configuration on intracellular lipid bilayers (Fig. 4D). Strikingly, the deletion of either residues 3 to 10 or residues 11 to 18 did not eliminate the ability of protein 6 to enhance MHV replication. Removal of these residues would be predicted to disrupt a helical membrane-bound hairpin and, less so, a molecule positioned parallel to the lipid bilayer or a transmembrane protein, since only 21 to 23 amino acids are required to cross the membrane and the hydrophobic part of protein 6 is approximately 34 amino acids. Deletion of residues 3 to 18 reduces the length of the hydrophobic stretch to a greater extent than either of the other two N-terminal deletions and results in inhibition of protein 6-mediated enhancement of MHV. Additional work will be required to determine the relationship of the structure of protein 6 to its function.

It is known that CoVs replicate on double-membrane vesicles (5, 17). Biochemical and microscopic studies showed that protein 6 is tightly associated with membranes and colocalizes with newly replicated viral RNA and replication machinery (10, 14, 16, 18). This, along with the fact that expression of the ORF6 gene by MHV results in more rapid emergence from the eclipse phase, with earlier expression of viral RNA and protein (16), raises the possibility that the protein functions as a nidus for the formation of sites of virus replication.

The ability to enhance MHV replication is not the only property of protein 6. Kopecky-Bromberg and coworkers have reported that protein 6 inhibits type 1 interferon induction and signaling pathways (9), suggesting a role for protein 6 in evasion of the innate immune response. Also, a recent report suggests that protein 6 is incorporated into the SARS-CoV virion (7), indicating that it functions additionally as a structural protein.

Collectively, these results suggest that protein 6 is involved in many processes in infected cells, in addition to possibly being a structural protein. Future work will be directed at determining how a protein of only 63 amino acids can possess so many properties yet can appear not to be critical for SARS-CoV viability or virulence (20).

This research was supported in part by a grant from the NIH (PO1 AI060699). J.N. and D.F. were supported by NIH training grants (T32 AI007533 and T32 HL07638, respectively).

REFERENCES

1. **Canfield, W. M., K. F. Johnson, R. D. Ye, W. Gregory, and S. Kornfeld.** 1991. Localization of the signal for rapid internalization of the bovine cation-independent mannose 6-phosphate/insulin-like growth factor-II receptor to amino acids 24–29 of the cytoplasmic tail. J. Biol. Chem. **266:**5682–5688.
2. **de Haan, C. A., L. Kuo, P. S. Masters, H. Vennema, and P. J. Rottier.** 1998. Coronavirus particle assembly: primary structure requirements of the membrane protein. J. Virol. **72:**6838–6850.
3. **Fleming, J. O., R. A. Shubin, M. A. Sussman, N. Casteel, and S. A. Stohlman.** 1989. Monoclonal antibodies to the matrix (E1) glycoprotein of mouse hepatitis virus protect mice from encephalitis. Virology **168:**162–167.
4. **Fleming, J. O., M. D. Trousdale, F. El-Zaatari, S. A. Stohlman, and L. P. Weiner.** 1986. Pathogenicity of antigenic variants of murine coronavirus JHM selected with monoclonal antibodies. J. Virol. **58:**869–875.
5. **Gosert, R., A. Kanjanahaluethai, D. Egger, K. Bienz, and S. C. Baker.** 2002. RNA replication of mouse hepatitis virus takes place at double-membrane vesicles. J. Virol. **76:**3697–3708.
6. **Harter, C., and I. Mellman.** 1992. Transport of the lysosomal membrane glycoprotein lgp120 (lgp-A) to lysosomes does not require appearance on the plasma membrane. J. Cell Biol. **117:**311–325.
7. **Huang, C., C. J. Peters, and S. Makino.** 2007. Severe acute respiratory syndrome coronavirus accessory protein 6 is a virion-associated protein and is released from 6 protein-expressing cells. J. Virol. **81:**5423–5426.
8. **Jadot, M., W. M. Canfield, W. Gregory, and S. Kornfeld.** 1992. Characterization of the signal for rapid internalization of the bovine mannose 6-phosphate/insulin-like growth factor-II receptor. J. Biol. Chem. **267:**11069–11077.
9. **Kopecky-Bromberg, S. A., L. Martinez-Sobrido, M. Frieman, R. A. Baric, and P. Palese.** 2007. SARS coronavirus open reading frame (ORF) 3b, ORF 6, and nucleocapsid proteins function as interferon antagonists. J. Virol. **81:**548–557.
10. **Kumar, P., V. Gunalan, B. Liu, V. T. Chow, J. Druce, C. Birch, M. Catton, B. C. Fielding, Y. J. Tan, and S. K. Lal.** 24 May 2007. The nonstructural protein 8 (nsp8) of the SARS coronavirus interacts with its ORF6 accessory protein. Virology [Epub ahead of print.] doi:10.1016/j.virol.2007.04.029.
11. **Kuo, L., G. J. Godeke, M. J. Raamsman, P. S. Masters, and P. J. Rottier.** 2000. Retargeting of coronavirus by substitution of the spike glycoprotein ectodomain: crossing the host cell species barrier. J. Virol. **74:**1393–1406.
12. **Nishimura, N., and W. E. Balch.** 1997. A di-acidic signal required for selective export from the endoplasmic reticulum. Science **277:**556–558.
13. **Ontiveros, E., L. Kuo, P. S. Masters, and S. Perlman.** 2001. Inactivation of expression of gene 4 of mouse hepatitis virus strain JHM does not affect virulence in the murine CNS. Virology **290:**230–238.
14. **Pewe, L., H. Zhou, J. Netland, C. Tangadu, H. Olivares, L. Shi, D. Look, T. M. Gallagher, and S. Perlman.** 2005. A severe acute respiratory syndrome-associated coronavirus-specific protein enhances virulence of an attenuated murine coronavirus. J. Virol. **79:**11335–11342.
15. **Snijder, E. J., P. J. Bredenbeek, J. C. Dobbe, V. Thiel, J. Ziebuhr, L. L. Poon, Y. Guan, M. Rozanov, W. J. Spaan, and A. E. Gorbalenya.** 2003. Unique and conserved features of genome and proteome of SARS-coronavirus, an early split-off from the coronavirus group 2 lineage. J. Mol. Biol. **331:**991–1004.
16. **Tangudu, C., H. Olivares, J. Netland, S. Perlman, and T. Gallagher.** 2007. Severe acute respiratory syndrome coronavirus protein 6 accelerates murine coronavirus infections. J. Virol. **81:**1220–1229.
17. **van der Meer, Y., E. J. Snijder, J. C. Dobbe, S. Schleich, M. R. Denison, W. J. Spaan, and J. K. Locker.** 1999. Localization of mouse hepatitis virus nonstructural proteins and RNA synthesis indicates a role for late endosomes in viral replication. J. Virol. **73:**7641–7657.
18. **von Brunn, A., C. Teepe, J. C. Simpson, R. Pepperkok, C. C. Friedel, R. Zimmer, R. Roberts, R. Baric, and J. Haas.** 2007. Analysis of intraviral protein-protein interactions of the SARS coronavirus ORFeome. PLoS ONE **2:**e459.
19. **Williams, M. A., and M. Fukuda.** 1990. Accumulation of membrane glycoproteins in lysosomes requires a tyrosine residue at a particular position in the cytoplasmic tail. J. Cell Biol. **111:**955–966.
20. **Yount, B., R. S. Roberts, A. C. Sims, D. Deming, M. B. Frieman, J. Sparks, M. R. Denison, N. Davis, and R. S. Baric.** 2005. Severe acute respiratory syndrome coronavirus group-specific open reading frames encode nonessential functions for replication in cell cultures and mice. J. Virol. **79:**14909–14922.